

# An Investigation of New Phase Diagram of $\text{Ag}_2\text{SO}_4 - \text{CaSO}_4$

Ravi V. Joat, Pravin S. Bodke, Shradha S. Binani, S. S. Wasnik

**Abstract**—A phase diagram of the  $\text{Ag}_2\text{SO}_4 - \text{CaSO}_4$  (Silver sulphate – Calcium Sulphate) binaries system using conductivity, XRD (X-Ray Diffraction Technique) and DTA (Differential Thermal Analysis) data is constructed. The eutectic reaction (liquid  $\rightarrow \alpha\text{-Ag}_2\text{SO}_4 + \text{CaSO}_4$ ) is observed at 10 mole%  $\text{CaSO}_4$  and  $645^\circ\text{C}$ . Room temperature solid solubility limit up to 5.27 mole % of  $\text{Ca}^{2+}$  in  $\text{Ag}_2\text{SO}_4$  is set using X-ray powder diffraction and scanning electron microscopy results. All compositions beyond this limit are two-phase mixtures below and above the transition temperature ( $\approx 416^\circ\text{C}$ ). The bulk conductivity, obtained following complex impedance spectroscopy, is found decreasing with increase in  $\text{CaSO}_4$  content. Amongst other binary compositions, the  $80\text{Ag}_2\text{SO}_4\text{-}20\text{CaSO}_4$  gave improved sinterability/packing density.

**Keywords**— $\text{Ag}_2\text{SO}_4\text{-CaSO}_4$  (Silver sulphate–Calcium Sulphate) binaries system, XRD (X-Ray Diffraction Technique) and DTA(Differential Thermal Analysis).

## I. INTRODUCTION

THE sulphate based solid electrolytes have found potential application in electrochemical devices [1], [2]. Particularly,  $\text{Li}_2\text{SO}_4$ ,  $\text{Na}_2\text{SO}_4$  and  $\text{Ag}_2\text{SO}_4$  based systems are potential materials from  $\text{SO}_x$  galvanic gas sensor viewpoint [2]. The first two materials have been studied extensively as compared to the latter one.

Amongst all the sulphates silver sulphate, a non-alkali metal is an exception that exhibits high  $\text{Ag}^+$  conductivity. The high ionic conductivity, in spite of large size of  $\text{Ag}^+$  ( $1.26\text{\AA}$ ), has been suggested to be due to its high quadrupolar polarizability. The  $\text{Ag}_2\text{SO}_4$  based solid electrolytes offer additional advantages from  $\text{SO}_x$  sensor application viewpoint [3]-[5]. Moreover, in these materials a major problem of cationic inter-diffusion between electrolyte and  $\text{Ag-Ag}_2\text{SO}_4$  solid reference electrode does not remain valid for creating concentration gradients and so better long-term sensor operation stability [6]-[8].

Silver sulphate is a polymorphs compound. It undergoes a phase transition from the high temperature high conducting hexagonal  $\alpha$ -phase (space group  $p63/mmc$ ) to the low

temperature moderately conducting orthorhombic  $\beta$ -phase (space group  $Fddd$ ) at  $418^\circ\text{C}$  [9]. The latter phase is isomorphous with the low temperature form of  $\text{Na}_2\text{SO}_4$  [10]. The electrical conductivity of pure  $\text{Ag}_2\text{SO}_4$  has been investigated in 1967 by Kvist [11]. In 1990 Liu et al have measured the ionic conductivity of  $\text{Me}_2\text{SO}_4$  ( $\text{Me} = \text{Li}, \text{Na},$  and  $\text{K}$ ) and  $\text{MSO}_4$  ( $\text{M} = \text{Sr}, \text{Ca}$  and  $\text{Ba}$ ) doped  $\text{Ag}_2\text{SO}_4$  and subsequently, tested for their utility in the  $\text{SO}_2$  gas sensor [12]. Electrical conductivity studies of mono-, di- and tri-valent cation doped  $\text{Ag}_2\text{SO}_4$  have indicated that besides the valance of guest cation its size and electronic configuration also play important role in conductivity [13].

The multiphase sulphate based systems have been preferred in  $\text{SO}_2$  gas sensor application due to their stable performance as compared to mono-phase. Moreover, the performance of sensor depends considerably on the magnitude of cationic conductivity, the phase and form along with the chemical and thermodynamical stability of solid electrolyte. Most of this information can easily be obtained from the binary-phase diagram and so they are important.

In 1907, Nacken has proposed the equilibrium phase diagrams of  $\text{Ag}_2\text{SO}_4$  with mono-valent alkali sulphates ( $\text{Me}_2\text{SO}_4$  where  $\text{Me} = \text{Na}$  and  $\text{K}$ ) using the results obtained towards thermal analysis [14]. In a systematic study, Takahashi et al have initially determined the conductivity and later constructed the binary phase diagrams with silver halides ( $\text{AgX-Ag}_2\text{SO}_4$ , where  $\text{X} = \text{Cl}$  and  $\text{Br}$ ) with the help of transport number, differential thermal analysis and x-ray powder diffraction techniques [15]. A detailed investigation on  $\text{Li}_2\text{SO}_4 - \text{Ag}_2\text{SO}_4$  binary phase diagram has been carried out by Oye [16]. Following an extensive work on  $\text{Ag}_2\text{SO}_4 - \text{Me}_2\text{SO}_4$  ( $\text{Me} = \text{Na}$  and  $\text{K}$ ) Secco et al., in recent past, have proposed  $\text{Ag}_2\text{SO}_4 - \text{Rb}_2\text{SO}_4$  binary phase diagram [17], [18]. According to these phase diagram  $\text{Ag}_2\text{SO}_4$  forms solid solution in entire compositional range of binary system. Whereas, in  $\text{Li}_2\text{SO}_4\text{-Ag}_2\text{SO}_4$  system very limited two-phase region is available.

It is evident from the literature that so far a systematic investigation on the  $\text{Ag}_2\text{SO}_4 - \text{MSO}_4$  ( $\text{M} = \text{Sr}, \text{Ca}, \text{Ba}$ ) binary systems, which may be potential from  $\text{SO}_x$  gas sensor viewpoint, is lacking. All these factors have prompted us to investigate  $\text{Ag}_2\text{SO}_4 - \text{CaSO}_4$  binary system, using electrical conductivity, differential scanning calorimetry, differential thermal analysis and x-ray powder diffraction techniques, constructing phase diagram to understand the phase and form of solid electrolyte belonging to this system in the vicinity of sensor operating temperature.

R. V. Joat is with the Department of Physics, Vidhya Bharati Mahavidyalaya, Amravati, PIN-444602, India (phone: +91-9422179298; e-mail: ravijoat@gmail.com).

P. S. Bodke is with the Department of Chemistry, Vidhya Bharati Mahavidyalaya, Amravati, PIN-444602, India (phone: +91-9823105999; e-mail: psbodke123@gmail.com).

S. S. Binani is with the Department of Chemistry, Vidhya Bharati Mahavidyalaya, Amravati, PIN- 444602, India (phone: +91-8055448934; e-mail: shradhabinani88@gmail.com).

S. S. Wasnik is with the Department of Physics, Vidhya Bharati Mahavidyalaya, Amravati, PIN- 444602, India.

## II. EXPERIMENTAL

The initial ingredients  $\text{Ag}_2\text{SO}_4$  and anhydrous  $\text{CaSO}_4$  with purity greater than 99.9% were procured from E Merck. The above chemicals in  $(100-x)\text{Ag}_2\text{SO}_4 - (x)\text{CaSO}_4$  (where  $x$ , -0.1, 2.5, 5.27, 7.57, 10, 20, ... 100) mole percent were mixed in an agate mortar under acetone for 2 hours. Well ground compositions were then transferred to translucent quartz ampoules and heated to the temperature  $20^\circ\text{C}$  above their respective melting point. The melt was allowed to cool, at the rate of  $1.50^\circ\text{C min}^{-1}$ , to room temperature. On the other hand, the compositions with more than 60-mole % of  $\text{CaSO}_4$  were prepared by fusing the well ground mixture at  $800^\circ\text{C}$  in silica ampoules so as to avoid thermal decomposition of silver sulphate. The ingots obtained by breaking the ampoules were finally pulverized to get fine powder. The entire procedure was carried out in a dark room so as to avoid photodecomposition of silver sulphate.

All samples were characterized using X-ray powder diffraction (XRD) (Philips PW 1700 diffractometer attached with PW 1710 controlling unit) using  $\text{CuK}\alpha$  radiation at room temperature. Whereas, XRD patterns were recorded at 300 and  $450^\circ\text{C}$  for a few selected samples viz. 20, 40 and 60 mole %  $\text{CaSO}_4$  added to  $\text{Ag}_2\text{SO}_4$ . In order to set the room temperature solid solubility limit, diffraction patterns were recorded for 5.27 mol%  $\text{CaSO}_4$  added to  $\text{Ag}_2\text{SO}_4$  samples prepared by two different techniques viz. (i) initial ingredients  $\text{Ag}_2\text{SO}_4$  and  $\text{CaSO}_4$  in appropriate mole ratio were thoroughly mixed mechanically under acetone for 2 hours and (ii) melting the same thoroughly mixed composition followed by slow cooling the melt to room temperature. The information towards the solid-solid phase transition temperature, the melting point and the heat of transition were obtained by differential scanning calorimetry (DSC) and differential thermal analysis using Mettler TA 4000 DSC 25 and Mettler TA DTA, respectively (under inert atmosphere) at a cooling rate of  $10^\circ\text{C min}^{-1}$ . The microstructures were examined with the help of scanning electron microscope (SEM) (Cambridge 250 mark - III stereoscan electron microscope).

The bulk conductivity of all samples, at various temperatures, was obtained following complex impedance spectroscopy as described elsewhere [19], [20].

## III. RESULTS AND DISCUSSION

### A. X-Ray Powder Diffraction (XRD)

A comparison of experimental  $d$  ( $\text{\AA}$ ) and relative intensity  $I/I_0$  of pure,  $94.73\text{Ag}_2\text{SO}_4-5.27\text{CaSO}_4$ ,  $93\text{Ag}_2\text{SO}_4-7\text{CaSO}_4$  and  $90\text{Ag}_2\text{SO}_4-10\text{CaSO}_4$  with those of the JCPDS (joint committee for powder diffraction standards) data of  $\text{Ag}_2\text{SO}_4$  and  $\text{CaSO}_4$  is given in Table I. It is seen that experimental characteristic  $d$  lines of mechanically mixed samples match closely with those of the JCPDS data for  $\text{Ag}_2\text{SO}_4$  and  $\text{CaSO}_4$ . On the other hand, all the experimental  $d$  values of  $94.73\text{Ag}_2\text{SO}_4-5.27\text{CaSO}_4$  sample prepared by melting are found to be in close agreement with those of JCPDS data for  $\text{Ag}_2\text{SO}_4$ . No line(s) corresponding to  $\text{CaSO}_4$  are seen in this composition. Similar results were found in the cases of  $\text{CaSO}_4$  lower than 5.27

mole% added to  $\text{Ag}_2\text{SO}_4$ . A close look at the Table I reveals appearance of a few weak characteristic lines corresponding to  $\text{CaSO}_4$  in case of  $93\text{Ag}_2\text{SO}_4-7\text{CaSO}_4$ . Furthermore, the number of characteristic lines due to  $\text{CaSO}_4$  and their relative intensity are found to be increasing with increase in its concentration in  $\text{Ag}_2\text{SO}_4$ .

In the X-ray powder diffraction results of two-phase mixture, the relative intensity ( $I/I_0$ ) values of each phase depend, more or less, on their concentration [21]. The absence of characteristic line(s) corresponding to  $\text{CaSO}_4$  for  $x = 5.27$  indicates the formation of a solid solution. Beyond this, all compositions are two-phase ( $\beta\text{-Ag}_2\text{SO}_4 + \beta\text{-CaSO}_4$ ) mixtures. The absence of any unidentified peak(s) rules out the possibility of formation of an intermediate phase in the entire binary system.

Notably, the high temperature XRD results revealed bi-phase mixtures of  $\beta\text{-Ag}_2\text{SO}_4 + \beta\text{-CaSO}_4$  and  $\alpha\text{-Ag}_2\text{SO}_4 + \beta\text{-CaSO}_4$  in the range from room temperature to  $416^\circ\text{C}$  and from  $416$  to  $600^\circ\text{C}$ , respectively. The lattice cell volume of  $\text{Ag}_2\text{SO}_4$ , within solid solubility limit, obtained from X-ray diffraction data is projected in Table II. As seen the cell volume decrease with increase in  $\text{CaSO}_4$  concentration indicating lattice contraction ( $\text{Ca}^{2+}$  is smaller than  $\text{Ag}^+$ ). These results endorse the formation of solid solution.

### B. Scanning Electron Microscopy (SEM)

The microstructure of 10, 20 and 30 mol%  $\text{CaSO}_4$  added to  $\text{Ag}_2\text{SO}_4$  clearly indicate the formation of two-phase mixture and in  $80\text{Ag}_2\text{SO}_4 - 20\text{CaSO}_4$  it shows denser packing as compared to other compositions.

### C. Thermal Analysis (DSC/DTA)

A typical DTA thermogram of  $80\text{Ag}_2\text{SO}_4-20\text{CaSO}_4$  is depicted in Fig. 1. The solid-solid phase transition temperature and the melting point are obtained from the onset of endothermic peak. It is worth mentioning here that the values of  $T_c$  obtained following DSC and DTA analyses for all samples were found in agreement within the accuracy of  $\pm 2^\circ\text{C}$ . Moreover, they were reproducible. A close look at the insert of Fig. 1 reveals a continuous decrease in the heat corresponding to solid-solid phase transition with an increase in  $\text{CaSO}_4$  concentration in  $\text{Ag}_2\text{SO}_4$ . This is due to the decrease in net content of latter in the samples indicating formation of two-phase mixtures.

A phase diagram of  $\text{Ag}_2\text{SO}_4\text{-CaSO}_4$  binary system, constructed using above XRD and DTA/DSC data is shown in Fig. 2. The solid circles represent the thermal discontinuities obtained from DTA/DSC. Thermodynamic features present in this binary system are summarized as follows, (a) the solid-solid phase transformation ( $\alpha\text{-Ag}_2\text{SO}_4 \rightarrow \beta\text{-Ag}_2\text{SO}_4$ ) and melting point for  $\text{Ag}_2\text{SO}_4$  are at  $416$  and  $658^\circ\text{C}$ , respectively, (b) the solid-solid phase transformation and melting point for  $\text{CaSO}_4$  are at  $1190$  and  $1450^\circ\text{C}$ , respectively, (c) eutectic reaction (liquid  $\rightarrow \alpha\text{-Ag}_2\text{SO}_4 + \text{CaSO}_4$ ) at 10 mole%  $\text{CaSO}_4$  and  $645^\circ\text{C}$  (d) approximately 5 mole%  $\text{CaSO}_4$  is soluble in  $\beta\text{-Ag}_2\text{SO}_4$  (e) two phase mixture of ( $\beta\text{-Ag}_2\text{SO}_4 + \beta\text{-CaSO}_4$ ) exists between room temperature and  $416^\circ\text{C}$ , (f) two phase mixture

of  $\alpha$ -Ag<sub>2</sub>SO<sub>4</sub> +  $\beta$ -CaSO<sub>4</sub> exists between 416 and 655°C for all compositions, (g) melt and solid  $\beta$ -CaSO<sub>4</sub> coexists beyond 30mole% CaSO<sub>4</sub> and above 655°C. Due to experimental limitation it was not possible to investigate thermal behaviour of samples above 1000°C. The dotted line is, however, an extrapolated liquidous curve.

A close look at this phase diagram reveals that  $T_c$  slightly decreases with an addition of CaSO<sub>4</sub> up to 7.5 mole% and thereafter it remains fairly constant. The initiatory decrease in  $T_c$  with an increase of CaSO<sub>4</sub> concentration is due to the formation of solid solution (Table I). Irvine and West have explained the decrease in  $T_c$  by assuming that the substitution of alio-valent cation results in the creation of extrinsic vacancies that causes lattice distortion/disorder [22]. According to them, the order-disorder phase transition in solid solution occurs more readily with rising temperature, and  $T_c$  displaces to a lower temperature.

#### D. Temperature Dependent Conductivity

The plots of  $\log(\sigma T)$  versus  $10^3/T$  for (x)Ag<sub>2</sub>SO<sub>4</sub>: (1-x)CaSO<sub>4</sub> system for  $x = 0-10$ ,  $v = 10-60$  and  $x = 70-100$  mole% are displayed in Figs. 3, 4 (a) and 4 (b), respectively. As seen, in both orthorhombic (stable below 416 °C) and hexagonal (stable above 416°C) modifications of Ag<sub>2</sub>SO<sub>4</sub> conductivity obey the Arrhenius law.

Observed change in conductivity at 416°C, for all samples, accounts for orthorhombic ( $\beta$ ) to hexagonal ( $\alpha$ ) phase transition in Ag<sub>2</sub>SO<sub>4</sub>. Notably, this temperature coincides with

the  $T_c$  obtained from DSC and DTA investigations. The change in slope in conductivity plot around 416°C, ascribed to switch in conduction mechanism due to structural phase-transition, is the manifestation of partial insolubility of CaSO<sub>4</sub> in Ag<sub>2</sub>SO<sub>4</sub> and vice-versa. Also, it rules out the formation of new intermediate compound in the entire binary system. These results are in agreement with above discussed XRD and DTA results. The conductivity measurements were restricted to below 560°C due to softening/deformation of samples at this temperature.

Insert of Figs. 3, 4 (a) and 4 (b) display the conductivity behavior (in both the modifications) of samples with CaSO<sub>4</sub> addition. In the high temperature modification (Fig. 3), the conductivity exhibits a maximum at 7.57 mole% ( $\approx$  7% vacancies) CaSO<sub>4</sub> within the solid solubility region. Whereas, in two-phase region (Figs. 4 (a) and (b)), it remains fairly invariant. In contrast, the conductivity below the transition temperature decreases (insert of Figs. 3, 4 (a) and 4 (b)).

The maximum in conductivity at 7.57 mole%, corresponding to  $\approx$  7% vacancies, is in good agreement with the reporting [23]. Since Ca<sup>2+</sup> (0.99Å) is smaller than Ag<sup>+</sup> (1.26 Å), the partial replacement of latter by former leads to an appreciable lattice contraction (Table II) in room temperature phase of Ag<sub>2</sub>SO<sub>4</sub>. Hence, Ca<sup>2+</sup> addition gives an additional vacancy with deeper potential well that offers large activation energy for Ag<sup>+</sup> migration. Therefore, as CaSO<sub>4</sub> content increases, conductivity decreases in low temperature phase.

TABLE I  
A COMPARISON OF EXPERIMENTAL X-RAY DIFFRACTION LINES WITH JCPDS FOR 5.27, 7 AND 10 MOLE % CaSO<sub>4</sub> ADDED TO Ag<sub>2</sub>SO<sub>4</sub>

Mechanical Mixed		Melt slow cooled				JCPDS				
5.27mole% Ca		5.27mole%Ca		7mole% Ca		10 mole% Ca				
<i>d</i>	<i>l/l<sub>0</sub></i>	<i>d</i>	<i>l/l<sub>0</sub></i>	<i>d</i>	<i>l/l<sub>0</sub></i>	<i>d</i>	<i>l/l<sub>0</sub></i>	<i>d</i>	<i>l/l<sub>0</sub></i>	Phase (hkl)
4.72	7	4.72	10	4.73	10	4.61	9	4.70	10	Ag <sub>2</sub> SO <sub>4</sub> (III)
4.00	8	3.99	23	4.01	20	3.95	21	3.99	25	Ag <sub>2</sub> SO <sub>4</sub> (220)
3.51	25	--	--	3.51	13	3.40	19	3.49	100	CaSO <sub>4</sub> (002)
3.18	48	3.18	76	3.18	85	3.15	82	3.17	10	Ag <sub>2</sub> SO <sub>4</sub> (040)
2.87	100	2.87	100	2.88	100	2.92	100	2.87	100	Ag <sub>2</sub> SO <sub>4</sub> (311)
2.65	36	2.65	68	2.65	64	2.54	78	2.64	90	Ag <sub>2</sub> SO <sub>4</sub> (022)
2.53	13	2.53	12	2.53	13	2.53	14	2.53	17	Ag <sub>2</sub> SO <sub>4</sub> (202)
2.42	11	2.42	26	2.43	21	2.42	25	2.42	30	Ag <sub>2</sub> SO <sub>4</sub> (033)
2.27	4	2.27	6	2.27	8	2.26	5	2.27	8	Ag <sub>2</sub> SO <sub>4</sub> (151)
2.20	6	--	--	2.20	1	2.20	4	2.20	20	CaSO <sub>4</sub> (212)
2.18	5	--	--	2.18	6	2.19	8	2.18	8	CaSO <sub>4</sub>
1.98	5	1.98	8	1.98	6	1.97	8	1.98	11	Ag <sub>2</sub> SO <sub>4</sub> (242)
1.95	4	--	--	1.95	5	1.94	7	1.95	8	Ag <sub>2</sub> SO <sub>4</sub> (260)
1.93	2	--	--	1.93	7	1.93	9	1.94	4	CaSO <sub>4</sub> (222)
1.92	14	1.92	34	1.92	23	1.92	20	1.92	30	Ag(351)
1.88	4	1.87	5	1.88	3	1.88	4	1.88	5	Ag(H3)
1.74	2	--	--	1.74	3	1.69	6	1.74	10	CaSO <sub>4</sub> (040)
1.71	9	1.71	13	1.71	12	1.75	13	1.71	17	Ag <sub>2</sub> SO <sub>4</sub> (062)

JCPDS card No. 27-1403 (Ag<sub>2</sub>SO<sub>4</sub>) and 6-0226 (CaSO<sub>4</sub>)

TABLE II  
COMPARISON OF EXPERIMENTAL LATTICE CELL CONSTANTS WITH JCPDS

Cell constants	JCPDS (Ag <sub>2</sub> SO <sub>4</sub> ) <sup>a</sup>	CaSO <sub>4</sub> doped Ag <sub>2</sub> SO <sub>4</sub>		
		$x = 00$	$x = 0.05$	$x = 0.0527$
a (Å)	10.2699	10.247	10.268	10.252
b (Å)	12.7069	12.693	12.679	12.625
c (Å)	759.25	758.32	758.32	740.08

JCPDS card number 27-1403 (Ag<sub>2</sub>SO<sub>4</sub>).

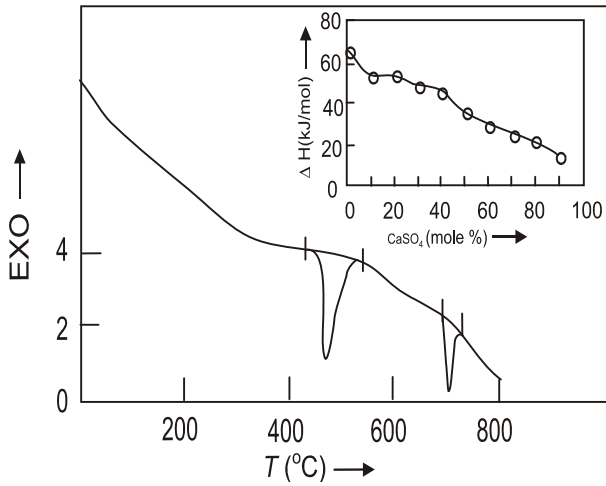


Fig. 1 DTA thermogram of 80  $\text{Ag}_2\text{SO}_4$ -20 $\text{CaSO}_4$  and insert variation of phase transition enthalpy with the addition of  $\text{CaSO}_4$  in  $\text{Ag}_2\text{SO}_4$

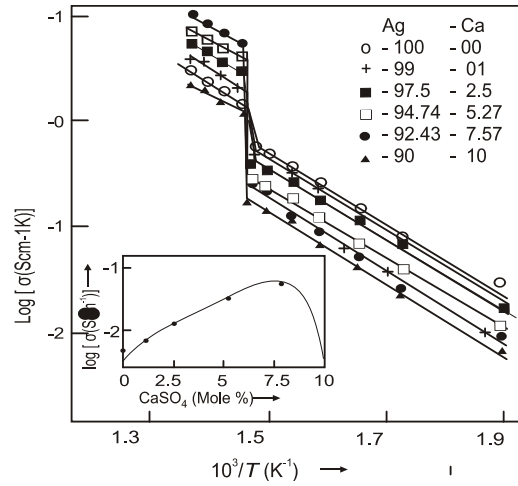


Fig. 3  $\log(\sigma T)$  versus  $1000/T$  for  $(1-x) \text{Ag}_2\text{SO}_4 - (x) \text{CaSO}_4$  where  $x = 0 - 10$ . Insert indicates the variation of conductivity with  $\text{CaSO}_4$  concentration

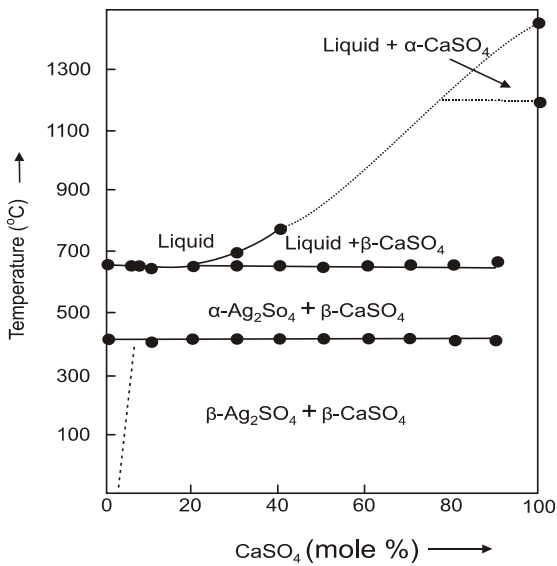


Fig. 2 The phase diagram for  $\text{Ag}_2\text{SO}_4$ - $\text{CaSO}_4$  binary system The solid circles represent thermal discontinuity as determined from differential thermal analysis. The indicated bi-phase regions are confirmed by x-ray diffraction. The broken line near  $\text{Ag}_2\text{SO}_4$  end indicates the uncertainty of the solid solution range in this phase. The dotted line is expected liquidous curve

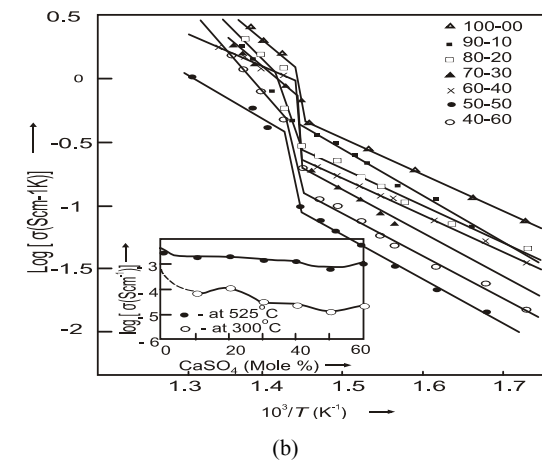
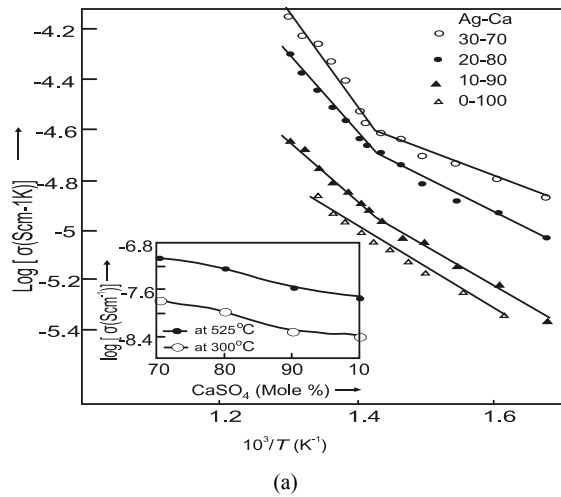


Fig. 4 (a)  $\log(\sigma T)$  versus  $1000/T$  for  $(1-x) \text{Ag}_2\text{SO}_4 - (x) \text{CaSO}_4$  binary system with (a)  $x = 10-60$  and (b)  $x = 70-100$ . Insert indicates variation of conductivity with  $\text{CaSO}_4$  concentration

## IV. CONCLUSION

The  $\text{CaSO}_4$  is sparingly soluble in both the hexagonal and the orthorhombic phases of  $\text{Ag}_2\text{SO}_4$  and form bi-phase mixtures in entire binary system. The eutectic reaction (liquid  $\rightarrow \alpha\text{-Ag}_2\text{SO}_4 + \text{CaSO}_4$ ) is observed at 10 mole%  $\text{CaSO}_4$  and  $645^\circ\text{C}$ . The value of conductivity although decreased but 20 mole %  $\text{CaSO}_4$  added to  $\text{Ag}_2\text{SO}_4$  is useful for Sox gas sensor application due to (i) its bi-phase nature at operating temperature, (ii) low activation enthalpy for ion migration, (iii) improved sinterability and (iv) good mechanical strength.

## ACKNOWLEDGMENT

Authors are thankful to the Principal, Vidyabharati Mahavidyalaya, Amravati for providing the laboratory facilities.

## REFERENCES

- [1] B. Heed, A. Lunden and K. Schroeder, 10<sup>th</sup> Intersoc Energy Conversion Engg. Conf, Aug(1975)p.613.
- [2] K. Singh and S. S. Bhoga, Bull Mater. Sci., 22 (1999) 71.
- [3] Q. G. Liu and W. L. Worrel, U.S. Pat, 303-320 (1981) 17.
- [4] W. L. Worrel and Q. G. Liu, J. Electroanal. Chem., 168 (1984) 355.
- [5] C. M. Mari, M. Beghi and S. Pizzini, Sensors and Actuators B, 2 (1990) 51.
- [6] H. Flood and N. Boye, Z. Electrochem., 66 (1962) 184.
- [7] D. M. Haaland, J. Electrochem. Soc., 127 (1980) 796.
- [8] Y. Saito, T. Maruyama, Y. Matsumoto, K. Kobayashi and Y. Yan, Solid State Ionics, 14(1984)273.
- [9] M. Kumari, E.A. Secco, Can. J. Chem. 56 (1978) 2616.
- [10] Y. Saito, T. Maruyama, Y. Matsumoto, K. Kobayashi, Thermochim Acta, 53 (1982) 289.
- [11] A. Kvist, Acta Universitat, Gothoburgensis 2 (1967).
- [12] Q. Liu, X. Sun and W. Wu, Solid State Ionics, 40-41 (1990) 465.
- [13] K. Singh, S. M. Pande, S. W. Anwane and S. S. Bhoga, J. Appl. Phys. A, 66(1998) 205.
- [14] R. Nacken, Neues Jahrb. Mineral. Geol, 24 (1907) 55.
- [15] T. Takahashi, E. Namura and O. Yamamoto, J. Appl. Electrochem, 2 (1972) 51.
- [16] H. A. Oye, Thesis (Technical University of Norway, Trondheim) 1963.
- [17] M. S. Kumari and E. A. Secco, Can. J. Chem. 61 (1983) 2804.
- [18] M. S. Kumari and E. A. Secco, Can. J. Chem. 63 (1985) 324.
- [19] K. Singh and S. S. Bhoga, Appl. Phys. A. 67 (1998) 475.
- [20] K. Singh and S. S. Bhoga, Proc. 4th National Seminar on Physics and Technology of Sensors, India, (1997) C23-.
- [21] K. Singh and S. S. Bhoga, J. Solid State Chem., 97 (1992) 141.
- [22] T. S. Irvin and A. R. West, Solid State Ionics. 28 (1988) 214.
- [23] H. H. Hoffer, W. Eysel and U. V. Alpen, J. Solid State Chem., 36 (1981) 365.